

FILM BOILING OF SMALL LIQUID DROPLETS
IN MOTION ON A HEATED SURFACE

By

DANIEL A. FORBES

Bachelor of Science

Oklahoma State University

Stillwater, Oklahoma

1967

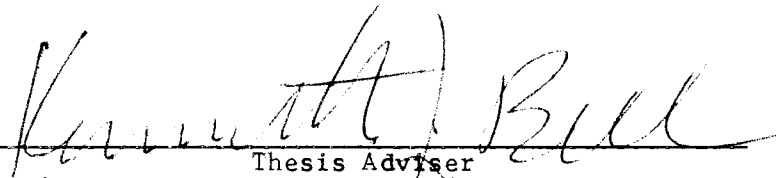
Submitted to the Faculty of the Graduate College
of the Oklahoma State University
in partial fulfillment of the requirements
for the Degree of
MASTER OF SCIENCE
July, 1968

Thesis
1968
FL 92 P
COPY 4

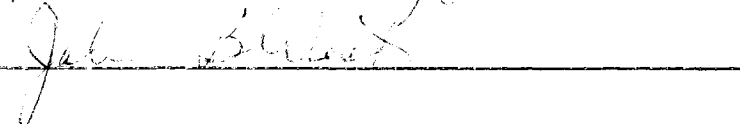
JAN 28 1969

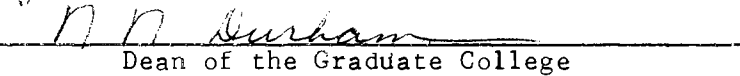
FILM BOILING OF SMALL LIQUID DROPLETS
IN MOTION ON A HEATED SURFACE

Thesis Approved:



Thesis Adviser





Dean of the Graduate College

696135

PREFACE

The velocity of small liquid masses in film boiling on a heated, inclined surface has been investigated. Droplet evaporation rate as a function of time on the surface and surface temperature has been determined. The results of theories in current literature have been compared to the results of the present experiments.

I am very much indebted to Professor Kenneth J. Bell for his advice and guidance during my thesis work and also for his friendship and patience. I would like to express my gratitude to the members of my graduate committee, fellow graduate students, and to the staff members of the School of Chemical Engineering.

Financial support was provided by a National Science Foundation Graduate Fellowship. Equipment funds were gratefully received from the United States Army Research Office in Durham, North Carolina.

I wish to acknowledge my indebtedness to my wife, Sheila, without whose constant support and encouragement my graduate studies would not have been possible.

TABLE OF CONTENTS

Chapter	Page
I. INTRODUCTION	1
II. EXPERIMENTAL APPARATUS	6
III. EXPERIMENTAL PROCEDURE	10
IV. DISCUSSION OF RESULTS.	13
V. CONCLUSIONS AND RECOMMENDATIONS.	25
A SELECTED BIBLIOGRAPHY	26
NOMENCLATURE.	27
APPENDIX A - CALIBRATIONS	29
APPENDIX B - ERROR ANALYSIS	32
APPENDIX C - RAW DATA	35
APPENDIX D - CALCULATED DATA.	45

LIST OF TABLES

Table	Page
I. Needle Calibrations with Water	30
II. Needle Calibrations with Benzene	31
III. Error Analysis	33
IV. Water Distance-Time Data	36
V. Benzene Distance-Time Data	37
VI. Water Evaporation Data for Full Tube Length.	38
VII. Benzene Evaporation Data	40
VIII. Water Evaporation Data for Intermediate Tube Lengths	41
IX. Total Evaporation Times for Stationary Droplets.	43
X. Water Evaporation Data for Full Tube Length.	46
XI. Water Evaporation Data for Intermediate Tube Lengths	48
XII. Benzene Evaporation Data	50

LIST OF FIGURES

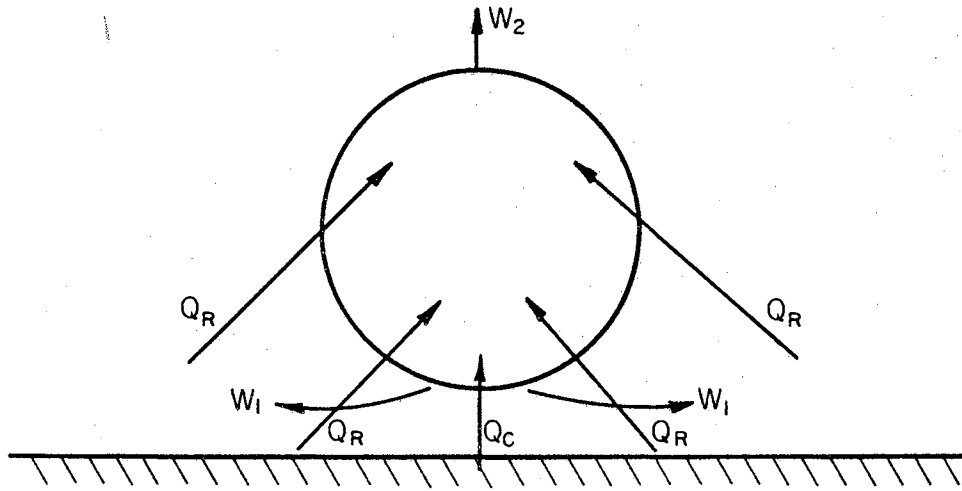
Figure	Page
1. Droplet Models.	2
2. Schematic of Apparatus.	7
3. Evaporation of Water Droplets	14
4. Intermediate Evaporation of Water Droplets.	15
5. Distance-Time Curves for Water (0.03874 gm)	18
6. Distance-Time Curves for Water (0.02893 gm)	19
7. Distance-Time Curves for Water (0.02113 gm)	20
8. Distance-Time Curves for Water (0.01368 gm)	21
9. Droplet Evaporation Times for Full Tube Length.	22
10. Total Evaporation Time for Water Droplets	24
11. Evaporation of Water Droplets (Uncorrected)	44

CHAPTER I

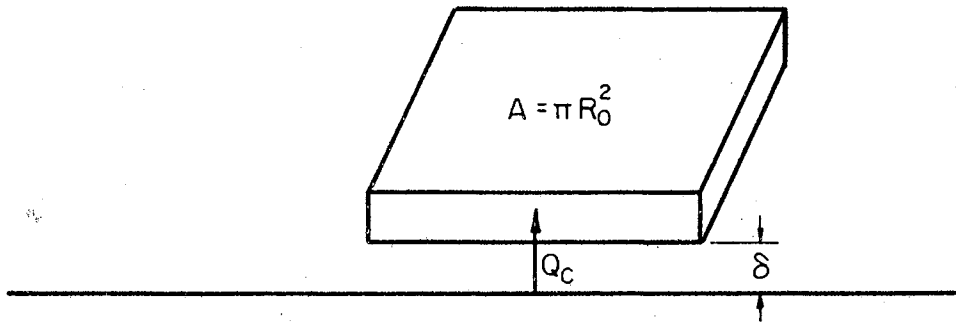
INTRODUCTION

The original reference to film boiling, published in 1756 by J. G. Leidenfrost (7), gave an account of the behavior of water droplets on a heated spoon. In honor of this original work, the term Leidenfrost Phenomenon has been applied to the film boiling of small liquid masses on a heated surface. Recent studies have also included the film boiling of large extended masses in referring to the Leidenfrost Phenomenon.

In the film boiling regime, the liquid masses are supported on a thin vapor film continuously generated by evaporation from the lower surface of the liquid. The masses are supported by the pressure gradient in the vapor flowing underneath the droplet. Studies by Baumeister (1), Gottfried, et al. (5), Lee (6), and Wachters (9) concern the analysis of the evaporation time for both small and extended stationary masses in film boiling. These studies include models of proposed mechanisms for heat transfer to the liquid, and for mass removal, and provide some indication of the conditions for stability of the Leidenfrost Phenomenon. Figure 1-(a) shows the heat and mass transfer paths for a stationary spherical droplet in film boiling (5). This model assumes that the vapor layer is generated by liquid evaporation from the lower surface. Heat is transferred by radiation (Q_r) to the entire outer surface of the droplet, and by conduction (Q_c) through the film. Mass removal occurs by evaporation into the vapor film on the lower surface (W_1) and by



(a) HEAT TRANSFER AND MASS TRANSFER PATHS FOR THE SPHERICAL DROPLET IN FILM BOILING.



(b) MODEL FOR DETERMINATION OF VELOCITY-DEPENDENT HEAT TRANSFER COEFFICIENT.

Figure 1. Droplet Models

molecular diffusion on the upper surface (W_2). The droplet is assumed isothermal at its saturation temperature. The vapor film is assumed to be superheated to a temperature halfway between saturation and the plate surface temperature. Surface roughness appears to affect the heat transfer rate to the drop as well as stability of the Phenomenon (4). The temperature difference between droplet and surface which gives the maximum evaporation time is presumed to be the minimum temperature at which stable film boiling can exist, and is termed the Leidenfrost point.

More recent studies have been concerned with the effect of relative motion between the liquid mass and the hot surface. The most recent is that of Baumeister and Schoessow (3), in which the evaporation times for droplets in film boiling on a moving surface are estimated by a direct integration of an energy balance on the droplet:

$$-\lambda e_L \frac{dV}{dt} = h_T(v) A(v) \Delta T \quad (1)$$

where the heat transfer coefficient, h_t , and drop area A are dependent on the liquid volume. The left hand side of equation (1) is the mass evaporation rate times the latent heat of vaporization. Equation (1) was rewritten in terms of dimensionless quantities, giving

$$-dV^* = h^* A^* dt^* \quad (2)$$

Baumeister and Schoessow assumed that the mechanism for energy transfer to the droplet was conduction across the vapor film (in creeping laminar flow) and radiation to the entire droplet surface. Diffusion from the upper surface and sides of the droplet was neglected. In addition, the droplet shape was assumed to be independent of velocity. Thus only the heat transfer coefficient is assumed to be velocity-dependent.

The model used by Baumeister and Schoessow for the derivation of the heat transfer coefficient is shown in Figure 1-(b). The drop is represented by a square shape, and a constant vapor film thickness is assumed beneath the drop. The resulting heat transfer coefficient is

$$h^* = \frac{h_s^*}{[(1+F)^{1/2} - F]^{1/2}} \quad (3)$$

where F is given by

$$F = (Pr \Phi)^{1/2} U^* \quad (4)$$

U^* is a dimensionless velocity given by the expression

$$U^* = \frac{U}{\left[4 \left(\frac{e_L}{e_g} - 1\right) g \left(\frac{\nu g_c}{e_L g}\right)^{1/2} \rho^*\right]^{1/2}} \quad (5)$$

Here, h_s^* represents the dimensionless heat transfer coefficient to a stationary drop in film boiling. h_s^* and other dimensionless expressions for stationary drops were developed in an earlier work (2). Before inserting the above expressions into the energy balance, the authors modified the F factor empirically, giving

$$F_n = (Pr \Phi)^{1/2} U^{*n} \quad (6)$$

The resulting expression for the total vaporization times of droplets in film boiling on a moving surface was

$$t^* = 2.23 (V^+)^{1/3} - .97 \quad (7)$$

where

$$V^+ = V^* \left[1 - \frac{F_n}{2(1-.25n)} + \frac{F_n^2}{8(1-.5n)} + \frac{B}{2.23(V^*)^{1/3}} \right]^3 \quad (8)$$

and

$$B = 1.1 \left[1 - \frac{F_n(.8)}{2(1-.4n)} + \frac{F_n^2(.8)}{8(1-.8n)} \right] - 2.07 \left(1 - \frac{F_n(.8)}{2(1-.25n)} + \frac{F_n^2(.8)}{8(1-.5n)} \right) + .97 \quad (9)$$

This expression was valid for droplets with initial volumes in the range $0.8 < V^* < 155$. When applied to water droplets, with $n = .25$, Baumeister and Schoessow found agreement within 7 per cent of experimental vaporization times.

Rester (8), in an initial study of which this work is a continuation, investigated the variables affecting the film boiling of a small liquid mass moving along a heated surface. These studies centered primarily upon determination of drag coefficients at terminal velocity.

The present work continues the studies initiated by Rester. The variables investigated are initial droplet size and surface temperature, and their effect upon droplet evaporation rates is to be determined.

CHAPTER II

EXPERIMENTAL APPARATUS

The apparatus is essentially that constructed by L. G. Rester (8). The heated surface is a longitudinally-split tube made from annealed 1-inch OD, 14 BWG stainless steel tube. The tube is mounted on transite cradles, which can be elevated to change the angle between the tube and the horizontal. A 10 foot scale was mounted alongside the tube to aid in measuring distances. Complete details of the tube mounting are in reference 8. A schematic diagram is shown in Figure 2.

The tube was modified by cutting out a slot 2-9/16 inches long by 3/8 inches wide in the tube 8 inches from the lower end. This slot was long enough that droplets at terminal velocity dropped through without hitting the far end of the slot, and could be caught in a plastic weighing bottle for determination of final mass after descent along various lengths of heated surface.

The tube is resistance-heated by current supplied by a Lincoln-weld SA-750 direct current generator. The tube circuit consists of the generator, the split tube (0.033 ohm resistance at 30°C.), and a 0.065 ohm water-cooled resistor in series with the tube. The field circuit of the generator was modified by adding in series a variable 93 ohm, 2 ampere rheostat. The rheostat in conjunction with the generator output controller gave the desired current control in a range of 100-350 amperes. The generator and tube were connected by No. 4/0 electrical

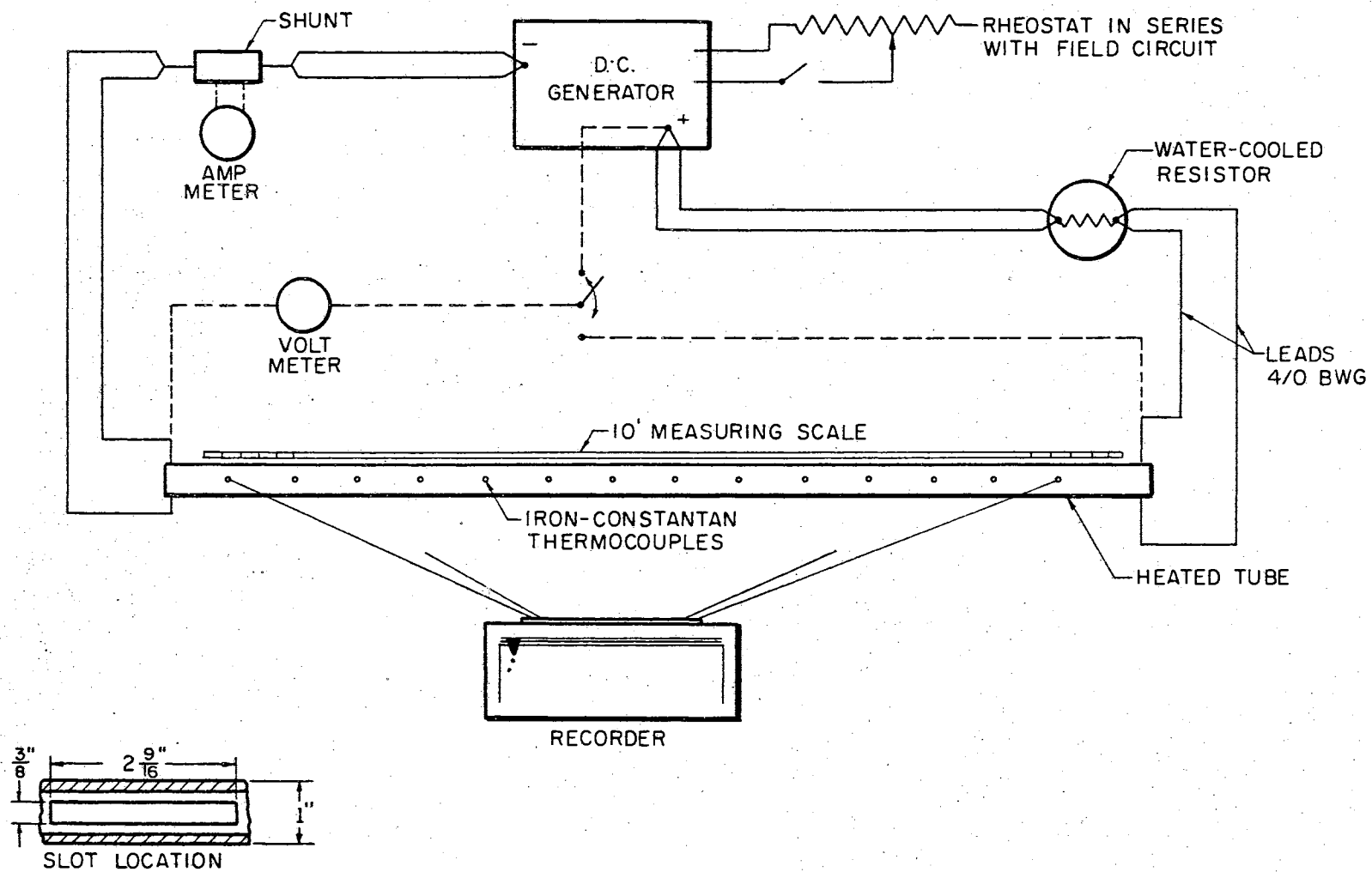


Figure 2. Schematic of Apparatus

leads. A shunt with 100 millivolt voltage drop at 1000 amperes was used with a Triplett Model 625 DC ammeter to measure current. Voltage was measured with a Triplett Model 625 DC voltmeter.

Tube temperatures were measured by eleven 20 BWG iron-constantan thermocouples. These were silver-soldered to the outside center of the tube, using a high-temperature silver solder with a melting point of 1500°F. Asbestos tape one-sixteenth of an inch thick was wrapped around each thermocouple where contact was made with the tube and continued along the thermocouple for three-fourths of an inch. In order to determine the temperature drop across the tube wall, several liquids were low nucleate-boiled in the tube. Comparison of the tube temperature and the boiling point of each liquid showed that the difference between tube and liquid temperature ranged from 1° at 100°C to an estimated 10° at 500°C. These differences were assumed to be estimates of the thermocouple errors for the temperature range considered.

An additional thermocouple was placed by the slot to determine the extent of additional heating caused by the greater current density at this point. The tube temperature along the slot varied from 30° higher than the average tube temperature at 325°C to 60° higher at 500°C. However, one inch above the slot the tube temperature was only 5° higher than the average tube temperature. Temperatures could be read directly by use of a Leeds and Northrup Speedomax W Multipoint Recorder.

The droplet-forming mechanism was a 5 ml. burette with a standard syringe adapter tip. Size 13, 15, 18, and 21 needles were used to deposit droplets on the tube surface. The needles were filed to square tips. Liquids used were distilled water and research-grade benzene. Initial droplet masses for each needle were found by calibrating 10

droplets from each needle. Each droplet was weighed in a plastic weighing bottle on a Mettler Model B6 Semi-Micro Balance. Balance accuracy was $\pm .02$ mg.

CHAPTER III

EXPERIMENTAL PROCEDURE

The principal variables considered in this investigation were surface temperature and initial droplet size. Accordingly, at the beginning of experimental work, the split tube was arbitrarily elevated to an angle of 4.79 degrees measured from the horizontal. This angle was checked periodically by cathetometer measurements to ensure that the supporting mechanism had not slipped.

Before heating, the tube was cleaned with emery paper, dusted, and then wiped with acetone-wetted Kimwipes. After starting cooling water flow in the water-cooled resistor, the DC generator controls were set for minimum output, and the generator was started. When the generator had been in operation for fifteen minutes, the electrode switch was turned to the "on" position. Power output was then gradually increased until the desired tube temperature was reached. This temperature was verified visually by observation of the recorder chart. Attainment of steady-state conditions required approximately thirty minutes. The tube temperature was found by averaging all thermocouple readings, with the exception of the end thermocouples. Average temperature variation along the tube was approximately $\pm 5^{\circ}\text{C}$. The approximate tube temperatures for these experiments were 325, 400, and 475°C .

While the tube was heating, the burette used for droplet formation was filled with the desired liquid, and the appropriate needle was

selected. The pinch-clamp used for controlling the rate of droplet formation was then opened until droplets slowly formed on the needle tip. The rate of droplet formation was then gradually increased until the weight of several droplets, collected and weighed at random, conformed to a calibration for that needle. In calibrating needles to determine a standard droplet size for each needle, the droplet size was found to be slightly dependent on the droplet formation rate. Consequently, an arbitrary formation rate of one droplet every two seconds was used, and each needle was calibrated for that rate. The calibrations are given in Appendix A. Standard deviations for these calibrations ranged from $1\frac{1}{2}$ to 2 per cent. When the rate of droplet formation had been set, the burette was then lowered into position above the heated tube until the needle tip was perpendicular to and approximately one-quarter inch above the tube surface.

Droplets were selected at random and timed for several different distances to determine droplet velocities. An electric timer with a hand switch was used. The timer was started as soon as the droplet contacted the tube surface, and was stopped when the droplet passed through the slot at the far end of the tube. Each droplet was timed for distances of 15, 35, 60, 85, and 105 inches. Time-distance data were taken for each initial droplet size and surface temperature.

Droplet evaporation was determined by the following procedure: The burette was set at the correct flow rate for the needle then in use. A droplet traveling down the tube was selected at random and caught in a plastic weighing bottle as it passed through the tube slot. Ten droplets were weighed for each initial droplet size and tube temperature. In order to reduce weighing error, the weighing bottle was handled only by

forceps, and was cleaned and dried with Kimwipes and then reweighed before another droplet was caught. Initially, the burette was located at the top of the tube and droplet evaporation was measured for the full tube length (105 inches). The burette was then moved down the tube toward the slot, and droplet evaporation was also measured for distances of 85, 60, 35, and 15 inches. Occasionally a droplet would move down the tube with a side-to-side motion. Weighings for these droplets were discarded.

Upon completion of the velocity and partial-evaporation experiments, the split tube was lowered to a horizontal position. Total evaporation times for stationary droplets were then found for each initial droplet size and tube temperature to determine possible effects of greater surface roughness and radiation heat transfer. The surface roughness was measured with a profilometer and found to average 80 microinches.

CHAPTER IV

DISCUSSION OF RESULTS

The effect of motion of a droplet in film boiling is an expected increase in evaporation rate by increasing both heat transfer to the bottom of the droplet and diffusional effects on the upper surface. Droplet evaporation was determined from experimental data for water droplets in motion for the full tube length (105"), and is shown in Figure 3. The curves presented in Figure 3 have been corrected for an estimated initial mass loss during impact of the droplet on the tube during deposition. The basis for this correction is shown in Figure 4. Droplet evaporation for intermediate distances was measured and is shown as a function of time on the tube. Extrapolation to zero time shows a probable initial mass loss which decreases with increasing temperature. The loss varies from approximately 3 per cent at 325°C to a projected 1 per cent at 475°C. Visual observation supported this viewpoint. At the lower tube temperatures, a mist of very small drops was formed during impact. The amount of mist was small, but was easily observable. Wachters (9) also observed this mist, and attributed it to small vapor bubbles which form during impact, move through the drop, and upon breaking through the upper surface form thin, unstable liquid jets which break apart, forming the observed mist. The maximum volume change during impact observed by Wachters was slightly less than 1 per cent for a polished gold-plated copper surface. However, he observed that by

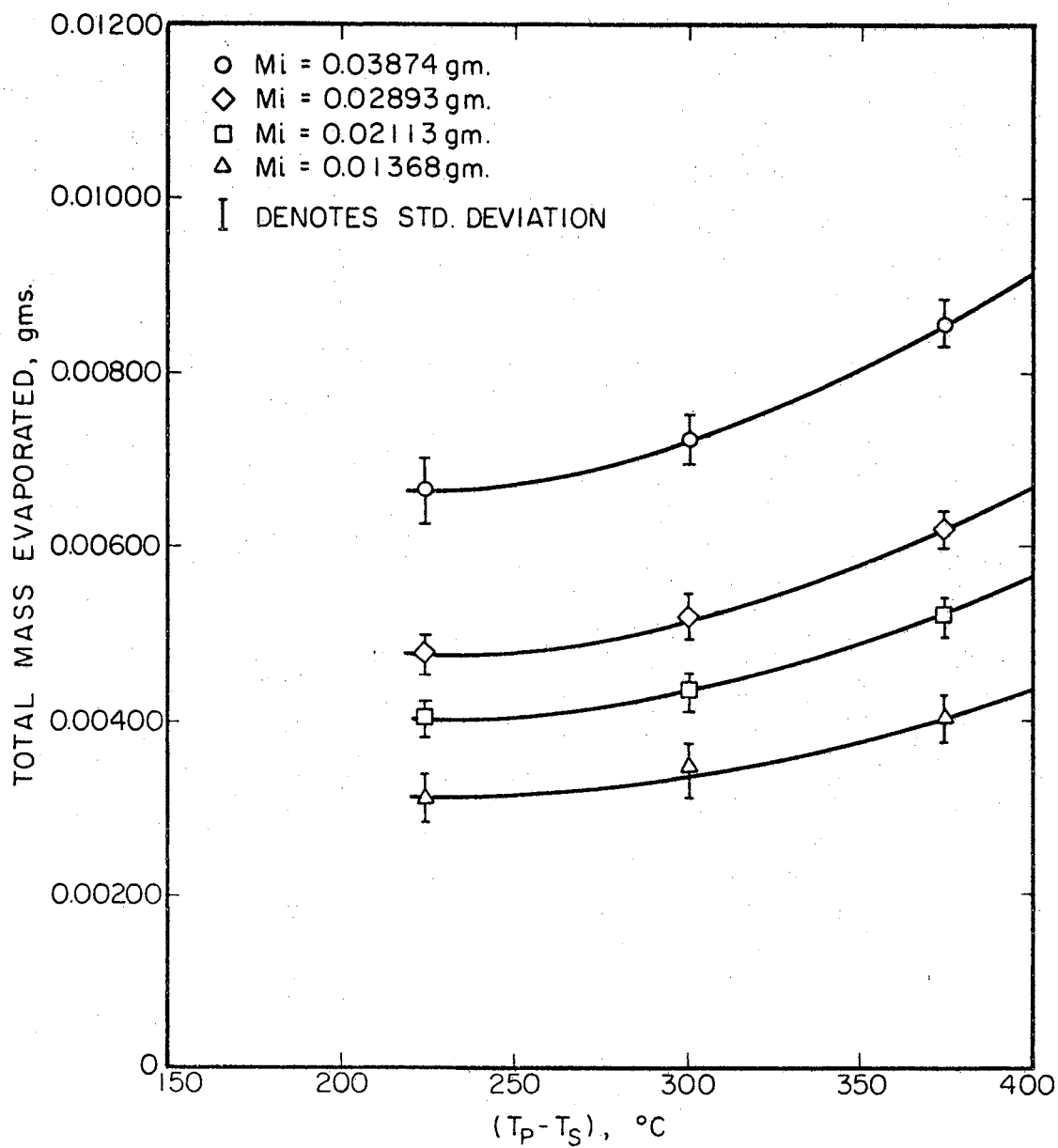


Figure 3. Evaporation of Water Droplets
(Full Tube Length)

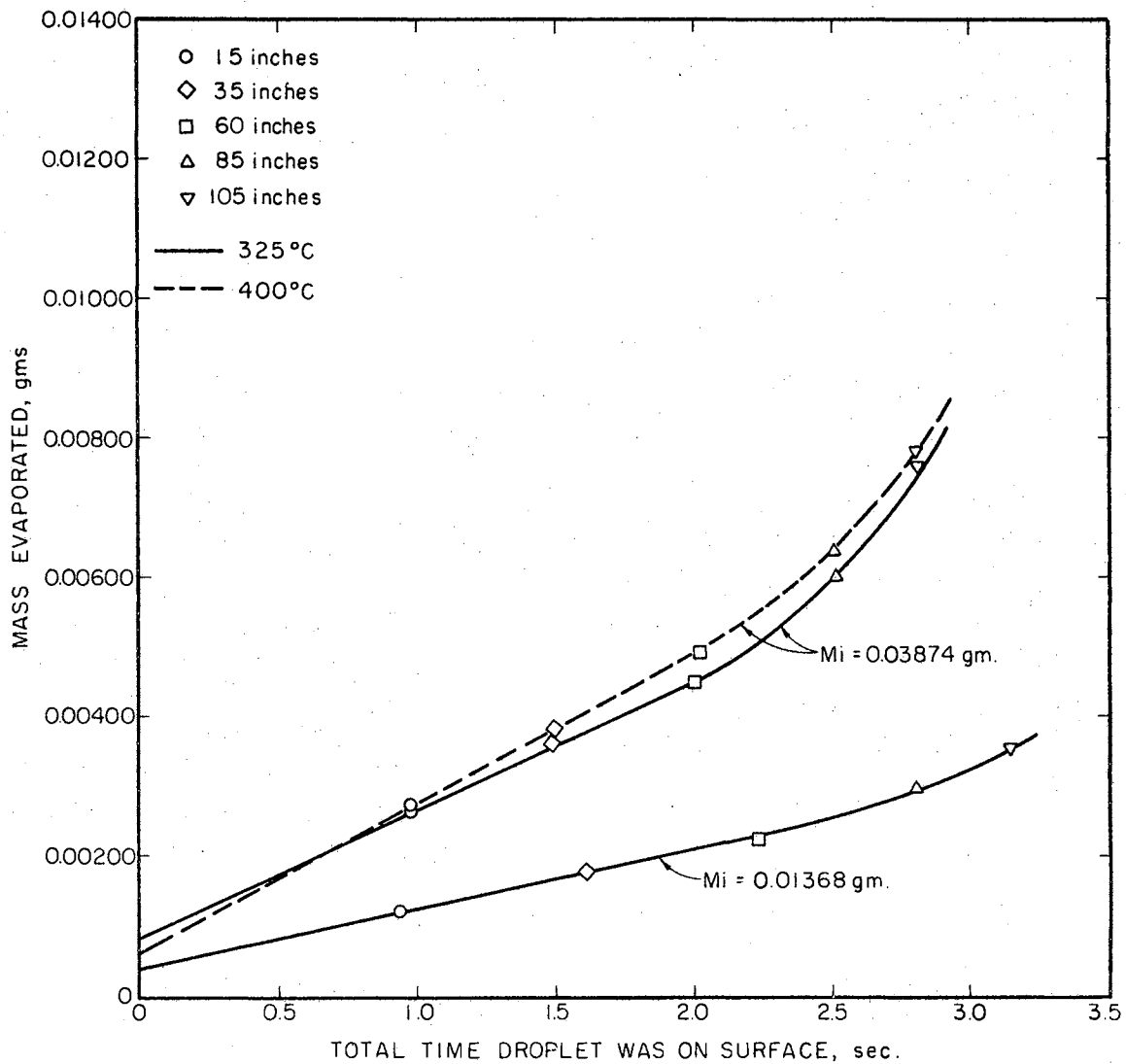


Figure 4. Intermediate Evaporation of Water Droplets

increasing the surface roughness, the maximum loss increased substantially. This corresponds to the results with the present surface.

The mist accounts for a portion of the estimated mass loss upon impact. In addition, some extremely minor loss can be attributed to initial formation of the vapor film.

The equations given by Baumeister and Schoessow (3), discussed in Chapter I, were re-integrated for an intermediate time interval to provide a theoretical comparison for the evaporation data now available. Again, the basic equation is

$$-dV^* = h^* A^* dt^* \quad (10)$$

For droplets with initial and final volumes in the range $0.8 < V^* < 155$, the dimensionless terms are related to V^* by

$$l^* = 0.8 (V^*)^{1/6} \quad (11)$$

$$A^* = 1.25 (V^*)^{5/6} \quad (12)$$

$$h_s^* = 1.075 (V^*)^{-1/6} \quad (13)$$

h^* is related to h_s^* by equation (3). Equation (10) reduces to

$$-dV^* \left[1 - \frac{Kn}{2(V^*)^{1/2}} + \frac{Kn^2}{8(V^*)^{3/4}} \right] \frac{1}{(V^*)^{2/3}} = 1.34 dt^* \quad (14)$$

where Kn is given by

$$\frac{(P_r \Phi)^{1/2} U^n}{\left[4 \left(\frac{e_L}{e_g} - 1 \right) g \left(\frac{g}{e_L g} \right)^{1/2} (0.8) \right]^{1/2}} \quad (15)$$

Integration of equation (14) between initial volume, V_i^* , and final volume, V_f^* , and between time, 0, and time, t^* , gives

$$\begin{aligned} (V_i^*)^{1/3} \left[1 - \frac{F_{in}}{2(1-.25n)} + \frac{F_{in}^2}{8(1-.5n)} \right] - (V_f^*)^{1/3} \left[1 - \frac{F_n}{2(1-.25n)} + \frac{F_n^2}{8(1-.5n)} \right] \\ = 0.446 t^* \end{aligned} \quad (16)$$

Velocities for calculation of the F factors were obtained for each initial droplet size from slopes of distance-time curves (Figures 5-8). These curves show that the effect of surface temperature on droplet velocity is minor. Equation (16) was used with experimental values for initial and final volumes to calculate the time each droplet should have been on the tube. Figure 9 shows the results, both for the theoretical value of n (n=1), and for the empirical value of 0.25 used by Baumeister and Schoessow. The predicted times are two to three times greater than the measured values. Trials with other values of n brought no significant improvement.

In their derivation of the velocity-dependent heat transfer coefficient, Baumeister and Schoessow used a square-shaped droplet. The data offered in support of their predictions consisted of droplets significantly larger ($V^* > 3.3$) than those considered in the present work. For extended droplets, a square model might be valid, but the droplets studied in this work are spherical or very nearly spherical. Also, the authors neglected diffusion effects. In these experiments, where the droplet itself is in motion through heated air, diffusion should have a more significant effect upon evaporation rates.

Surface roughness was not considered in the above derivation. A well-polished surface has an rms roughness on the order of 2-4 micro-inches. This roughness is about 1 per cent of the vapor film thickness for a stationary droplet. The average surface roughness for the split tube used in these experiments was 80 microinches. The effect of

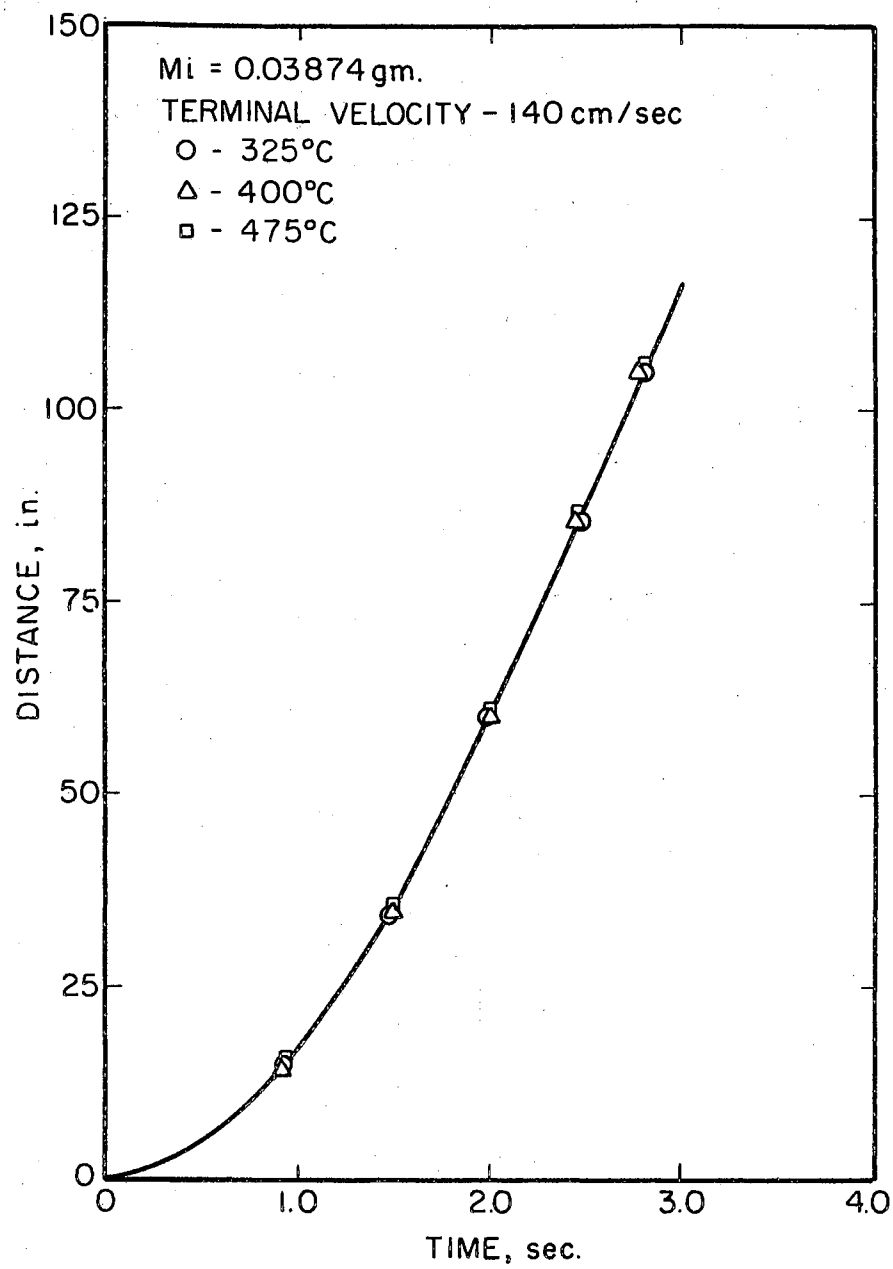


Figure 5. Distance-Time Curves for Water
(0.03874gm)

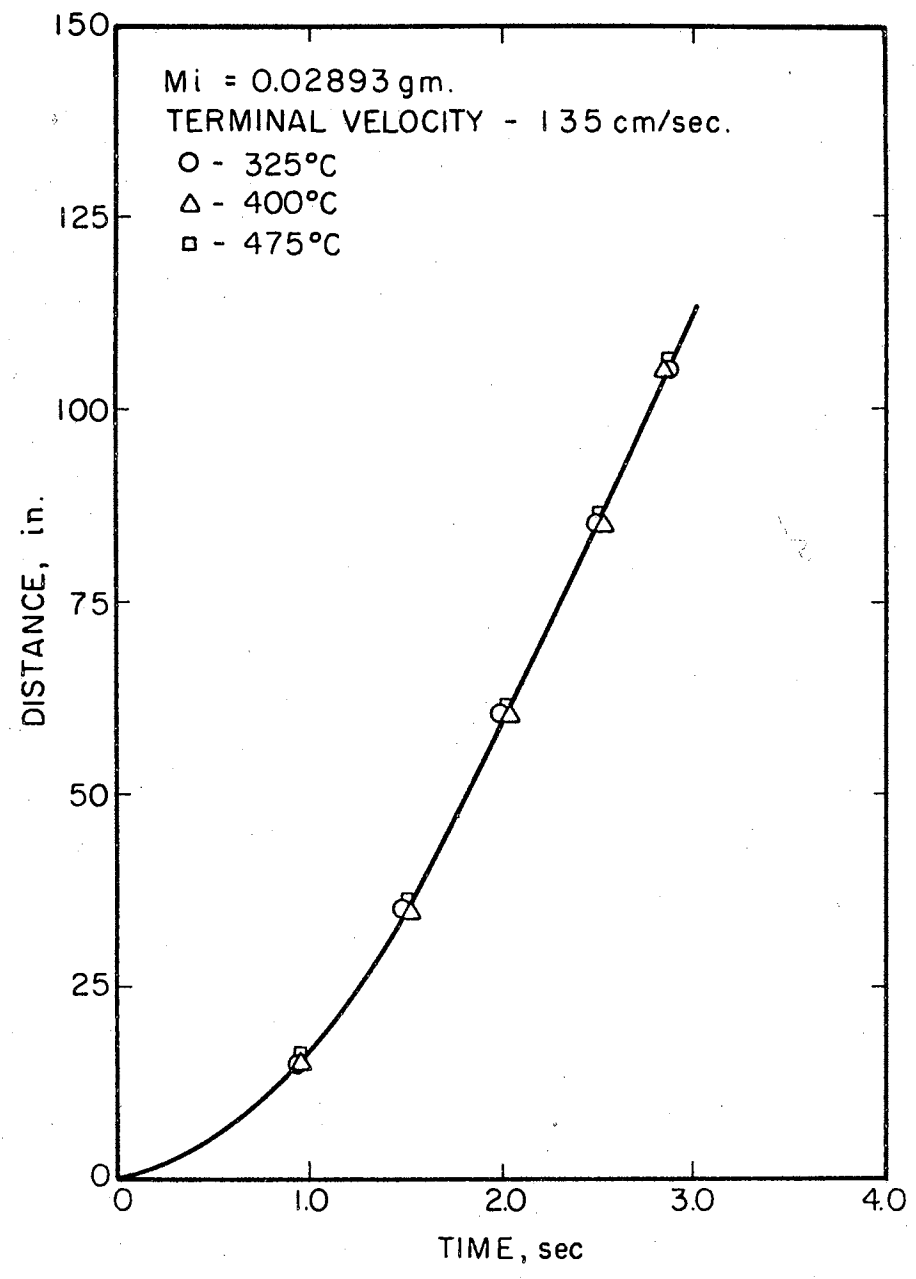


Figure 6. Distance-Time Curves for Water (0.02893gm)

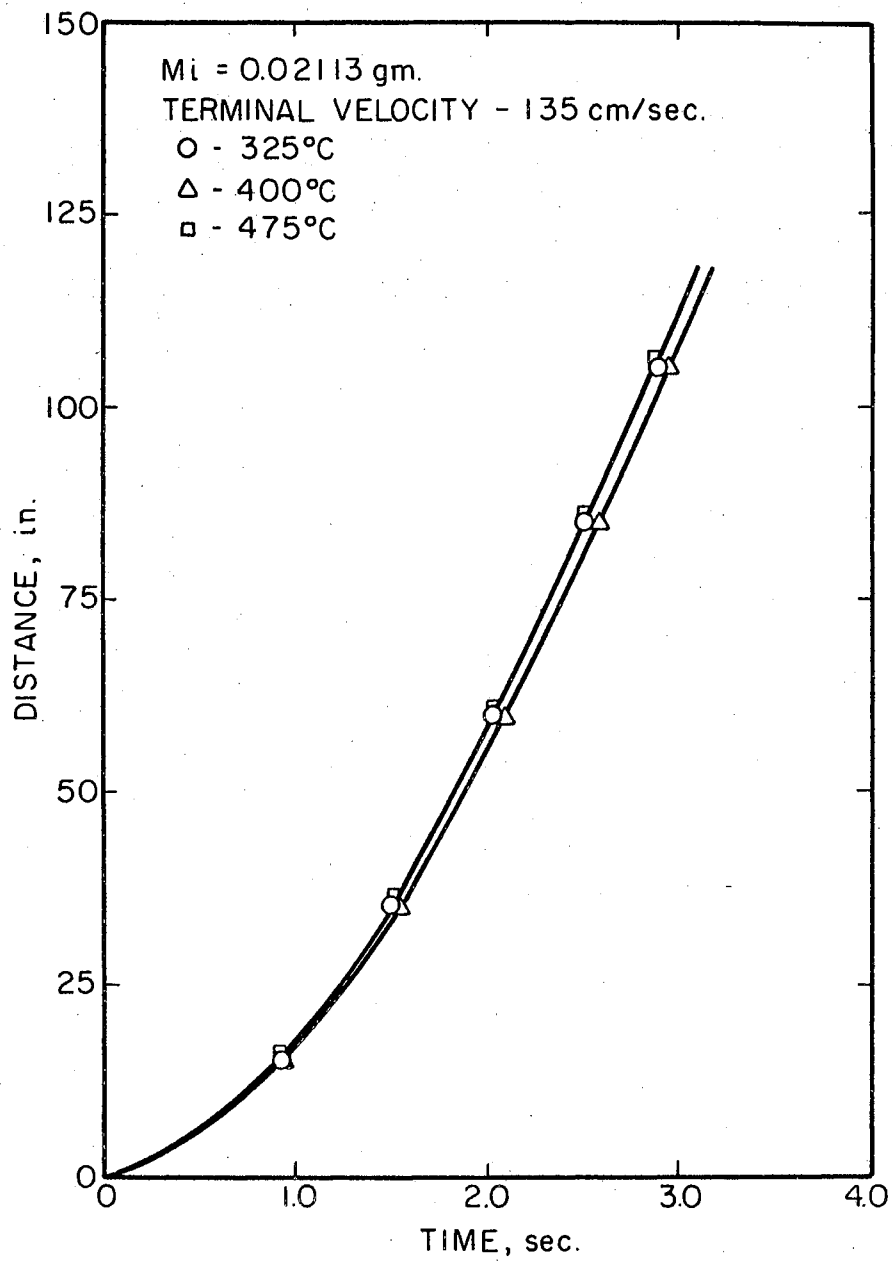


Figure 7. Distance-Time Curves for Water
(0.02113gm)

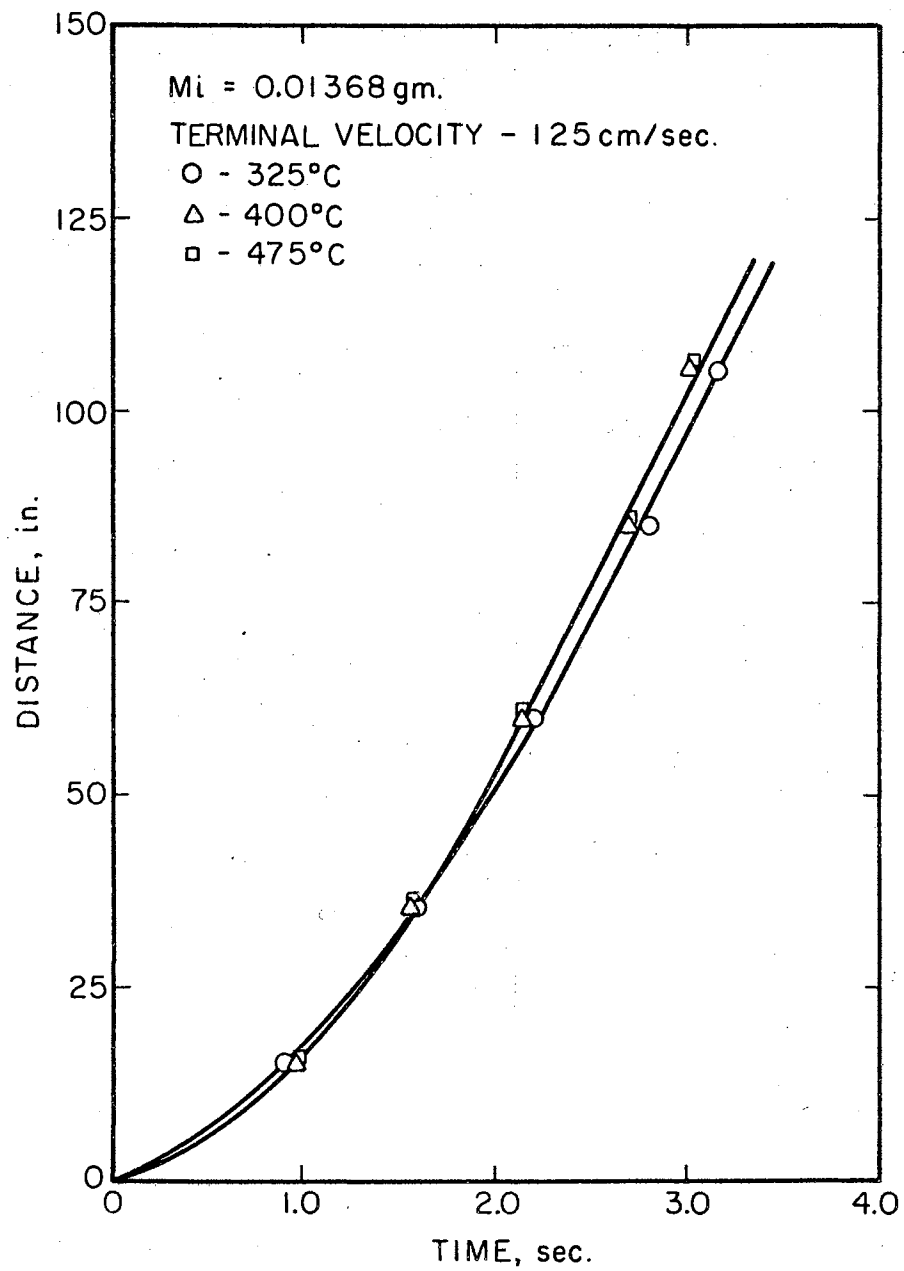
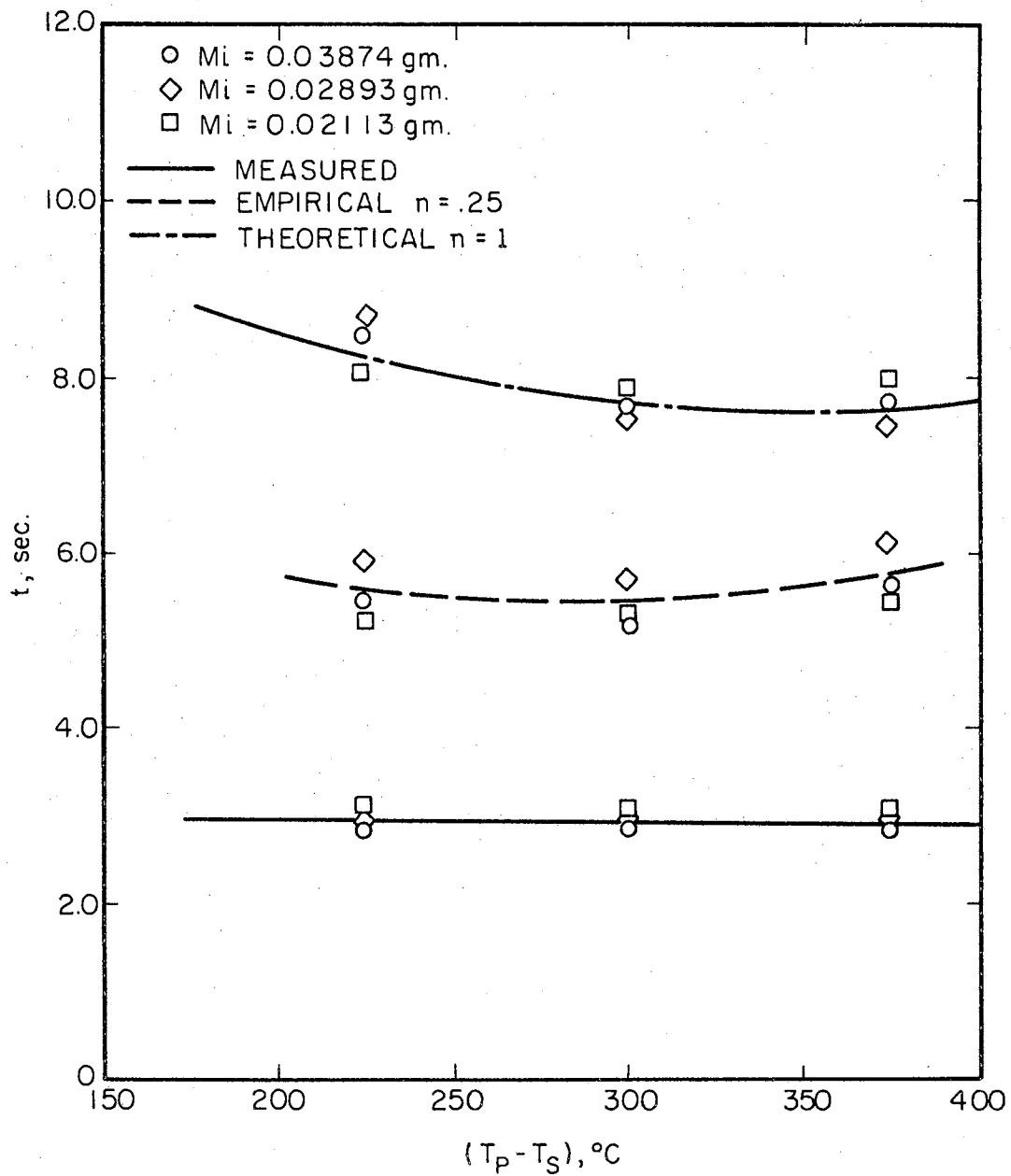


Figure 8. Distance-Time Curves for Water
(0.01368gm)



EMPIRICAL AND THEORETICAL VALUES ARE FROM MODIFIED BAUMEISTER EQ.

$$(V_i^*)^{1/3} \left(1 - \frac{F_{in}}{(1-.25n)(2)} + \frac{F_{in}^2}{8(1-.5n)} \right) - (V_f^*)^{1/3} \left(1 - \frac{F_n}{2(1-.25n)} + \frac{F_n^2}{8(1-.5n)} \right) = .446t^*$$

Figure 9. Droplet Evaporation Times for Full Tube Length

surface roughness should be more significant when relative motion exists between droplet and heated surface, where the expected effect of such motion would be a decrease in the effective vapor film thickness.

Total evaporation times were also determined for stationary water droplets on the split tube in a horizontal position (Figure 10). These are approximately 25 per cent less than those reported by Lee (6). This difference can be attributed to the increased surface roughness over that reported by Lee, and to increased radiation heat transfer due to the increased view factor offered by the walls of the heated tube, compared to a flat plate.

The tube length was too short to allow measurements of total evaporation times for moving droplets. However, these could be roughly estimated by assuming a mean evaporation rate for total evaporation. The estimated times for water droplets in motion were 15-20 per cent of the equivalent evaporation times previously reported for stationary droplets (6). These estimates are also included in Figure 10. A limited amount of data was taken for benzene as a measure of the consistency of the water data (Appendix C).

All of the experiments involving evaporation of moving droplets were conducted under unsteady state conditions, with each droplet starting at rest and accelerating to its terminal velocity. The measured evaporation rates should be somewhat less than those for a droplet moving at the terminal velocity for the full time interval under consideration.

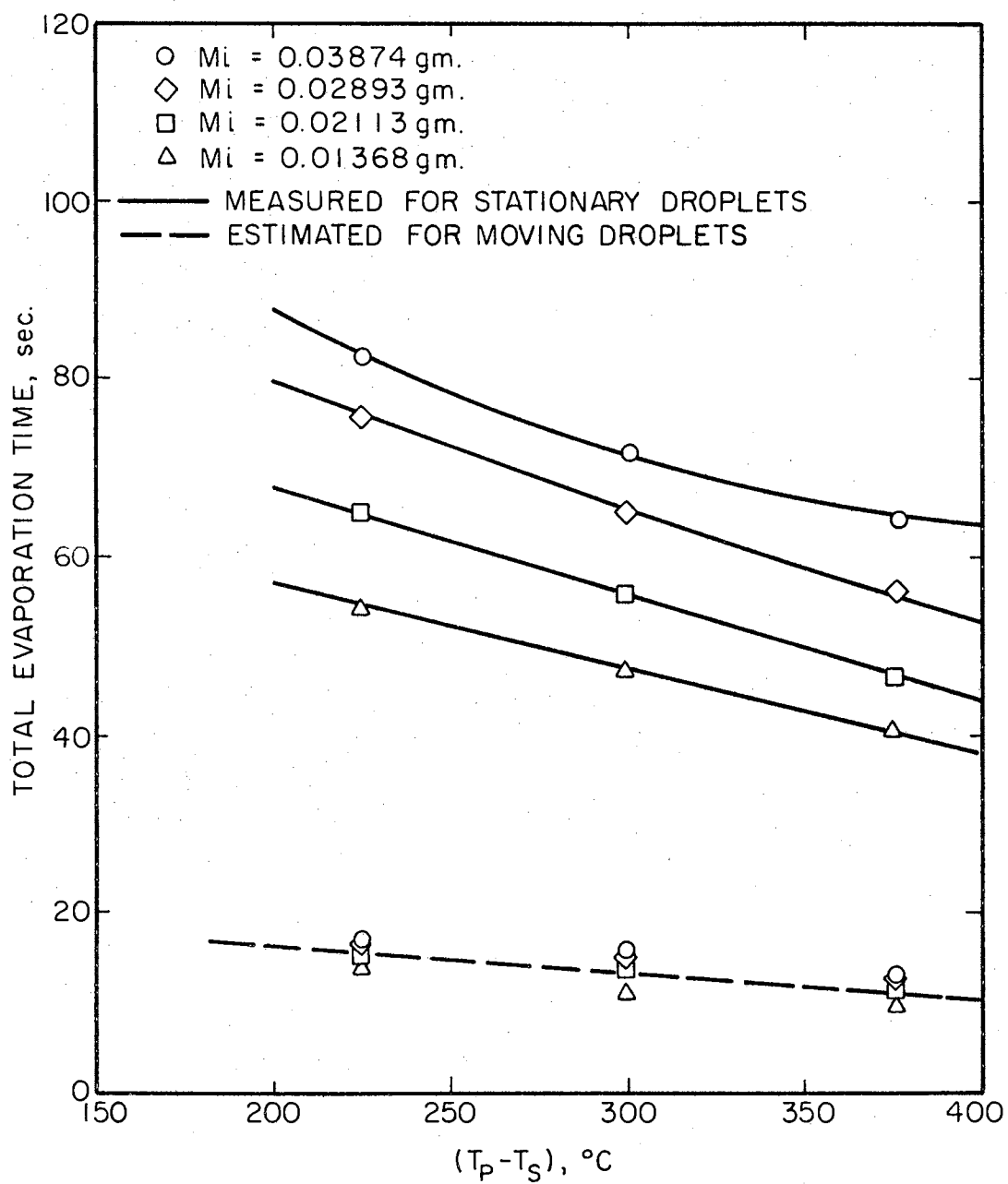


Figure 10. Total Evaporation Time for Water Droplets

CHAPTER V

CONCLUSIONS AND RECOMMENDATIONS

The following significant conclusions are supported by these experiments:

- (1) Droplet evaporation rates are significantly increased when relative motion exists between droplet and heated surface.
- (2) The heat transfer coefficient for a moving droplet appears to be more dependent upon surface roughness than that for a stationary droplet.

The following recommendations are made after considering the results of this investigation:

- (1) Surfaces with various roughnesses should be used for a complete study of the effect of surface conditions on heat transfer to a moving droplet.
- (2) A model should be developed which includes the effects of diffusion and surface roughness.
- (3) A method of measuring the vapor film thickness for a moving droplet should be developed.

A SELECTED BIBLIOGRAPHY

1. Baumeister, K. J., "Heat Transfer to Water Droplets on a Flat Plate in the Film Boiling Regime," Ph.D. Thesis, University of Florida (1964).
2. Baumeister, K. J., T. D. Hamill, and G. J. Schoessow, "A Generalized Correlation of Vaporization Times of Drops in Film Boiling on a Flat Plate," Proc. 3rd Int. Heat Transfer Conference, Vol. IV, 66-73 (August, 1966).
3. Baumeister, K. J., and G. J. Schoessow, "A Creeping Flow Solution of Leidenfrost Boiling with a Moving Surface," Paper submitted to the 10th National Heat Transfer Conference, August 11-14, 1968, Philadelphia, Pennsylvania.
4. Bradfield, W. S., "Liquid-Solid Contact in Stable Film Boiling," IEC Fund. Quart. V, 2, 200-204 (May, 1966).
5. Gottfried, B.S., C. J. Lee, and K. J. Bell, "The Leidenfrost Phenomenon: Film Boiling of Liquid Droplets on a Flat Plate," Int. Jour. Heat Mass Transfer, 9, 1167-1188 (November, 1966).
6. Lee, C. J., "A Theoretical and Experimental Investigation of the Leidenfrost Phenomenon for Small Droplets," Ph.D. Thesis, Oklahoma State University (1965).
7. Leidenfrost, J.G., *De Aquae Communis Nonnullis Qualitatibus Tractatus*, ("A Tract About Some Qualities of Common Water"), Duisburg (1756). (An English translation of the original treatise appeared in Int. Jour. Heat Mass Transfer 9, 1153-1156, November, 1966.)
8. Rester, L. G., "A Study of the Convective Leidenfrost Phenomenon," M.S. Thesis, Oklahoma State University (1968).
9. Wachters, L. H. J., "Heat Transfer from a Hot Wall to Drops in a Spheroidal State," Laboratorium voor Fysische Technologie, Technische Hogeschool, Delft, The Netherlands.

NOMENCLATURE

- A area of droplet, cm^2
- A* dimensionless area of lower surface $A^* = \frac{A}{\left(\frac{\sigma g_c}{\epsilon_L g}\right)}$
- C_p specific heat at constant pressure, $\text{cal}/(\text{g})(^\circ\text{K})$
- F dimensionless function defined by equation (4)
- F_n dimensionless function defined by equation (6)
- f radiation factor $1/\left[1 + \frac{2hr}{4hc\left(1 + \frac{2}{20} \frac{\sigma_p \Delta T}{\lambda}\right)}\right]^3$
- g acceleration of gravity, $980 \text{ cm}/\text{sec}^2$
- g_c gravitational constant (conversion constant between mass and force units), $1.0 \text{ gm-cm}/(\text{sec}^2)(\text{dyne})$
- h_c conductive heat transfer coefficient $h_c = 1.075 \left(\frac{k^3 \lambda^* g^{1/2} \epsilon_L^{1/2} e_v \sigma^{1/2} g_c^{1/2}}{\Delta T \mu (V_{\text{average}})^{2/3}}\right)^{1/4}$
 $\text{cal}/(\text{sec})(\text{cm}^2)(^\circ\text{K})$
- h^* dimensionless heat transfer coefficient
- h_r radiation heat transfer coefficient $h_r = \frac{\epsilon_L \bar{\sigma} (T_p^4 - T_s^4)}{\Delta T}$
 $\text{cal}/(\text{sec})(\text{cm}^2)(^\circ\text{K})$
- h_s^* dimensionless heat transfer coefficient for a stationary droplet
- h_t total heat transfer coefficient, $\text{cal}/(\text{sec})(\text{cm}^2)(^\circ\text{K})$
- k thermal conductivity of vapor, $\text{cal}/(\text{cm})(\text{sec})(^\circ\text{K})$
- l^* dimensionless average drop thickness $l^* = l / \left(\frac{\sigma g_c}{\epsilon_L g}\right)^{1/2}$
- l average drop thickness $l = \frac{V}{\pi r_{\text{max}}^2 a}$, cm
- n empirical correction exponent
- Pr Prandtl Number $C_p \mu / k$
- T temperature, $^\circ\text{K}$
- T_p plate or tube temperature, $^\circ\text{C}$
- T_s saturation temperature, $^\circ\text{C}$

T temperature difference, $T_p - T_s$, °C

t time, sec

t* dimensionless time $t^* = \frac{t}{f} \left[\frac{\lambda^4 e_L^{3/2} \sigma^{5/2} g_c^{5/2} \mu}{k^3 \lambda^* g^{1/2} (e_L - e_g) e_g \Delta T^3} \right]^{1/4}$

U velocity of plate relative to drop, cm/sec

U* dimensionless velocity

V volume of drop, cm^3

V* dimensionless volume of drop $V^* = V / \left[\frac{\sigma g_c}{e_L g} \right]^{3/2}$

Greek Letters

δ vapor film thickness, cm

ϵ_L liquid emissivity, dimensionless

λ latent heat of vaporization, cal/g

λ^* modified heat of vaporization $\lambda^* = \lambda \left(1 + \frac{7}{20} \frac{C_p \Delta T}{\lambda} \right)^{-3}$, cal/g

μ viscosity of vapor, g/(cm)(sec)

e_g vapor density, g/(cm^3)

e_L liquid density, g/(cm^3)

σ surface tension, dyne/cm

\bar{F} Boltzmann constant, $4.876 \cdot 10^{-9}$ cal/(cm^2)(hr)(°K)⁴

Φ latent to sensible heat ratio $\Phi = \frac{\lambda^*}{C_p \Delta T}$

APPENDIX A

CALIBRATIONS

TABLE I
NEEDLE CALIBRATIONS WITH WATER
(73 °F)

Needle Size Gage	Drop Mass gms	Deviation From Mean Per Cent	Needle Size Gage	Drop Mass gms	Deviation From Mean Per Cent
13	0.03940	+1.70	15	0.02845	-1.66
	0.03935	+1.57		0.02935	+1.45
	0.03855	-0.49		0.02900	+0.24
	0.03895	+0.54		0.02835	-2.00
	0.03950	+1.95		0.02870	-0.80
	0.03905	+0.80		0.02910	+0.59
	0.03875	+0.03		0.02860	-1.14
	0.03790	-2.17		0.02925	+1.11
	0.03795	-2.04		0.02895	+0.07
	<u>0.03930</u>	+1.45		<u>0.02955</u>	+2.14
	0.03874		0.02893		
Standard deviation	1.47%		Standard Deviation	1.19%	
18	0.02160	+2.22	21	0.01395	+1.97
	0.02135	+1.04		0.01355	-0.95
	0.02065	-2.27		0.01330	-2.78
	0.02070	-2.03		0.01355	-0.95
	0.02125	+0.57		0.01390	+1.61
	0.02155	+1.99		0.01330	-2.78
	0.02125	+0.57		0.01385	+1.24
	0.02085	-1.32		0.01380	+0.88
	0.02070	-2.03		0.01375	+0.51
	<u>0.02145</u>	+1.51		<u>0.01380</u>	+0.88
	0.02113		0.01368		
Standard deviation	1.68%		Standard deviation	1.65%	

TABLE II
NEEDLE CALIBRATIONS WITH BENZENE
(72°F)

Needle Size Gage	Drop Mass gms	Deviation From Mean Per Cent	Needle Size Gage	Drop Mass gms	Deviation From Mean Per Cent
13	0.01460	+0.14	15	0.01130	-1.57
	0.01470	+0.82		0.01145	-0.26
	0.01400	-3.98		0.01160	+1.05
	0.01460	+0.14		0.01145	-0.26
	0.01490	+2.19		0.01185	+3.22
	0.01425	-2.26		0.01165	+1.48
	0.01445	-0.89		0.01135	-1.13
	0.01460	+0.14		0.01160	+1.05
	0.01470	+0.82		0.01120	-2.44
	<u>0.01500</u>	+2.88		<u>0.01135</u>	-1.13
	0.01458			0.01148	
Standard deviation	1.91%		Standard deviation	1.61%	
18	0.00825	+1.43	21	0.00600	+1.86
	0.00850	+1.55		0.00585	-0.68
	0.00835	-0.24		0.00585	-0.68
	0.00820	-2.03		0.00580	-1.53
	0.00870	+3.94		0.00610	+3.56
	0.00830	-0.84		0.00560	-4.92
	0.00815	-2.63		0.00595	+1.01
	0.00840	+0.35		0.00570	-3.22
	0.00825	-1.43		0.00595	+1.01
	<u>0.00860</u>	+2.74		<u>0.00605</u>	+2.73
	0.00837			0.00589	
Standard deviation	2.03%		Standard deviation	2.12%	

APPENDIX B

ERROR ANALYSIS

TABLE III
ERROR ANALYSIS

Variable Measured or Calculated	Maximum Relative Error	Magnitude of Variable at Condition of Maximum Relative Error	Maximum Relative Error, %
Tube Inclination	0.12°	4.790°	2.5
Droplet Mass	0.00014 gm.	0.00560 gm.	2.5
Tube Temperature	9°C	475°C	1.9
Distance	1/32 in.	15 in.	0.2
Droplet Evaporation	0.00026 gm.	0.00393 gm.	6.6
Droplet Timings	0.06 sec.	2.19 sec.	2.7
Terminal Velocity	6 cm/sec.	135 cm/sec.	4.6
Total Evaporation Time for Stationary Droplet	2 sec.	55 sec.	3.6
Calculated Time for Droplet on Tube Surface	0.4 sec.	5.45 sec.	7.3

The effects of errors in the measured variables were considered in the calculations previously discussed. Errors in initial and final droplet masses, surface temperatures, and terminal velocities had a cumulative effect upon the calculated times, resulting in the relatively greater errors for these calculations (Table III). Errors involved in measuring tube inclination, distance traveled along the tube, and the time each droplet was on the tube surface, had no effect on other measured or calculated values.

The errors shown for initial and final droplet masses, and for droplet evaporation were evaluated statistically, and in each case represent the greatest standard deviation observed for that variable. Ten droplets were weighed for each initial and final mass, and the resulting values for droplet evaporation should represent a reasonably good statistical picture.

APPENDIX C

RAW DATA

TABLE IV

WATER DISTANCE-TIME DATA
(4.790°)

Mass, gm. 0.03874	Distance inches	Average Time, sec.	Mass, gm. 0.02893	Distance, inches	Average Time, sec.	Mass, gm. 0.02113	Distance, inches	Average Time, sec.
Temp., °C	15	0.97	Temp., °C	15	0.99	Temp., °C	15	0.94
325	35	1.49	325	35	1.51	325	35	1.59
	60	1.99		60	2.02		60	2.16
	85	2.50		85	2.52		85	2.73
	105	2.80		105	2.90		105	3.11
0.01368	15	0.93	0.03874	15	0.98	0.02893	15	0.98
	35	1.61		35	1.48		35	1.52
327	60	2.24	400	60	2.02	401	60	2.05
	85	2.80		85	2.51		85	2.54
	105	3.16		105	2.83		105	2.89
0.02113	15	0.95	0.01368	15	0.96	0.03874	15	0.98
	35	1.55		35	1.60		35	1.49
400	60	2.10	400	60	2.15	473	60	2.00
	85	2.61		85	2.70		85	2.48
	105	2.96		105	3.01		105	2.81
0.02893	15	0.97	0.02113	15	0.96	0.01368	15	0.96
	35	1.51		35	1.55		35	1.59
473	60	2.02	473	60	2.11	473	60	2.15
	85	2.54		85	2.60		85	2.68
	105	2.90		105	2.93		105	2.99

TABLE V
 BENZENE DISTANCE-TIME DATA
 (4.790°)

Mass, gm.	Distance, inches	Average Time, sec.	Mass, gm.	Distance, inches	Average Time, sec.	Mass, gm.	Distance, inches	Average Time, sec.
0.01458			0.01148			0.00837		
Temp., °C	15	0.95	Temp., °C	15	1.00	Temp., °C	15	1.01
326	35	1.53	326	35	1.54	326	35	1.59
	60	2.03		60	2.11		60	2.21
	85	2.53		85	2.70		85	-
	105	2.97		105	-		105	-
0.00589	15	1.03						
	35	1.65						
326	60	2.33						
	85	-						
	105	-						

TABLE VI

WATER EVAPORATION DATA FOR FULL TUBE LENGTH (105")

Initial Mass gm.	Final Drop gm.	Initial Mass gm.	Final Drop gm.	Initial Mass gm.	Final Drop gm.	Initial Mass gm.	Final Drop gm.
0.03874		0.02893		0.02113		0.01368	
Temp., °C	0.03110	Temp., °C	0.02340	Temp., °C	0.01650	Temp., °C	0.01010
323	0.03050	324	0.02400	324	0.01670	323	0.00990
	0.03140		0.02315		0.01642		0.00985
	0.03140		0.02325		0.01620		0.01045
	0.03145		0.02350		0.01660		0.01010
	0.03120		0.02290		0.01675		0.01040
	0.03150		0.02335		0.01680		0.01005
	0.03120		0.02354		0.01635		0.01010
	0.03090		0.02398		0.01650		0.00975
0.03874		0.02893		0.02113		0.01368	
	0.03090		0.02340		0.01635		0.00980
400	0.03125	400	0.02325	400	0.01625	401	0.01000
	0.03120		0.02305		0.01615		0.00975
	0.03050		0.02330		0.01650		0.00990
	0.03070		0.02305		0.01595		0.01010
	0.03085		0.02345		0.01610		0.00970
	0.03075		0.02375		0.01625		0.00985
	0.03105		0.02280		0.01640		0.00990
	0.03070		0.02310		0.01630		0.00965
	0.03100		0.02300		0.01645		0.01015

Table VI (Continued)

Initial Mass gm.	Final Drop gm.	Initial Mass gm.	Final Drop gm.	Initial Mass gm.	Final Drop gm.	Initial Mass gm.	Final Drop gm.
0.03874		0.02893		0.02113		0.01368	
Temp., °C 472	0.02980	Temp., °C 472	0.02250	Temp., °C 472	0.01595	Temp., °C 472	0.00950
	0.02975		0.02220		0.01570		0.00935
	0.02990		0.02265		0.01580		0.00940
	0.02960		0.02205		0.01555		0.00925
	0.02955		0.02235		0.01540		0.00920
	0.02940		0.02245		0.01535		0.00950
	0.03000		0.02205		0.01555		0.00945
	0.02980		0.02250		0.01565		0.00930
	0.02965		0.02225		0.01560		0.00935
	0.02985		0.02260		0.01545		0.00970

TABLE VII

BENZENE EVAPORATION DATA

Initial Mass gm.	Final Drop gm. (105")	Initial Mass gm.	Final Drop gm. (85")	Initial Mass gm.	Final Drop gm. (60")	Initial Mass gm.	Final Drop gm. (60")
0.01458		0.01148		0.00937		0.00589	
Temp., °C 325	0.00475	Temp., °C 324	0.00525	Temp., °C 324	0.00375	Temp., °C 324	0.00255
	0.00510		0.00508		0.00430		0.00240
	0.00495		0.00470		0.00415		0.00240
	0.00475		0.00492		0.00410		0.00230
	0.00545		0.00519		0.00390		0.00260
	0.00460		0.00530		0.00425		0.00270
	0.00480		0.00508		0.00440		0.00225
	0.00500		0.00486		0.00405		0.00255
	0.00470		0.00497		0.00395		0.00240
	0.00515		0.00536		0.00435		0.00235

TABLE VIII

WATER EVAPORATION DATA FOR INTERMEDIATE TUBE LENGTHS

Initial Mass gm.	Final Drop gm.	Initial Mass gm.	Final Drop gm.	Initial Mass gm.	Final Drop gm.	Initial Mass gm.	Final Drop gm.
0.03874	(85")	0.03874	(60")	0.03874	(35")	0.03874	(15")
Temp., °C 325	0.03270 0.03255 0.03275 0.03245 0.03240 0.03280 0.03275 0.03265 0.03270 0.03250	Temp., °C 324	0.03420 0.03430 0.03415 0.03405 0.03445 0.03395 0.03410 0.03400 0.03420 0.03425	Temp., °C 323	0.03515 0.03500 0.03495 0.03535 0.03520 0.03510 0.03530 0.03500 0.03505 0.03525	Temp., °C 323	0.03605 0.03580 0.03630 0.03575 0.03600 0.03615 0.03590 0.03610 0.03595 0.03620
0.01368	(85")	0.01368	(60")	0.01368	(35")	0.01368	(15")
326	0.01060 0.01075 0.01055 0.01050 0.01065 0.01055 0.01045 0.01080 0.01070 0.01065	326	0.01135 0.01160 0.01145 0.01125 0.01150 0.01155 0.01120 0.01140 0.01130 0.01135	325	0.01190 0.01170 0.01200 0.01175 0.01195 0.01180 0.01190 0.01185 0.01190 0.01205	326	0.01240 0.01255 0.01235 0.01240 0.01245 0.01230 0.01250 0.01235 0.01245 0.01238

TABLE VIII (Continued)

Initial Mass gm.	Final Drop gm.	Initial Mass gm.	Final Drop gm.	Initial Mass gm.	Final Drop gm.	Initial Mass gm.	Final Drop gm.
0.03874	(85")	0.03874	(60")	0.03874	(35")	0.03874	(15")
Temp., °C 400	0.03230	Temp., °C 400	0.03380	Temp., °C 400	0.03475	Temp., °C 400	0.03600
	0.03245		0.03395		0.03515		0.03625
	0.03220		0.03360		0.03485		0.03585
	0.03200		0.03355		0.03470		0.03595
	0.03235		0.03365		0.03510		0.03610
	0.03215		0.03350		0.03475		0.03615
	0.03210		0.03345		0.03495		0.03595
	0.03240		0.03385		0.03480		0.03610
	0.03205		0.03375		0.03500		0.03590
	0.03225		0.03390		0.03505		0.03605

TABLE IX

TOTAL EVAPORATION TIMES FOR STATIONARY DROPLETS
(HORIZONTAL TUBE)

Liquid	H ₂ O	H ₂ O	H ₂ O	H ₂ O	H ₂ O	H ₂ O	H ₂ O	H ₂ O
Initial Mass, gms.	0.03874	0.02893	0.02113	0.01368	0.03874	0.02893	0.02113	0.01368
Average Time, sec.	82	75	64	54	71	65	55	46
Temp., °C	325	325	325	325	400	400	400	400
Liquid	H ₂ O	H ₂ O	H ₂ O	H ₂ O	C ₆ H ₆	C ₆ H ₆		
Initial Mass, gms.	0.03874	0.02893	0.02113	0.01368	0.01458	0.00589		
Average Time, sec.	63	55	46	41	18	13		
Temp., °C	475	475	475	475	325	325		

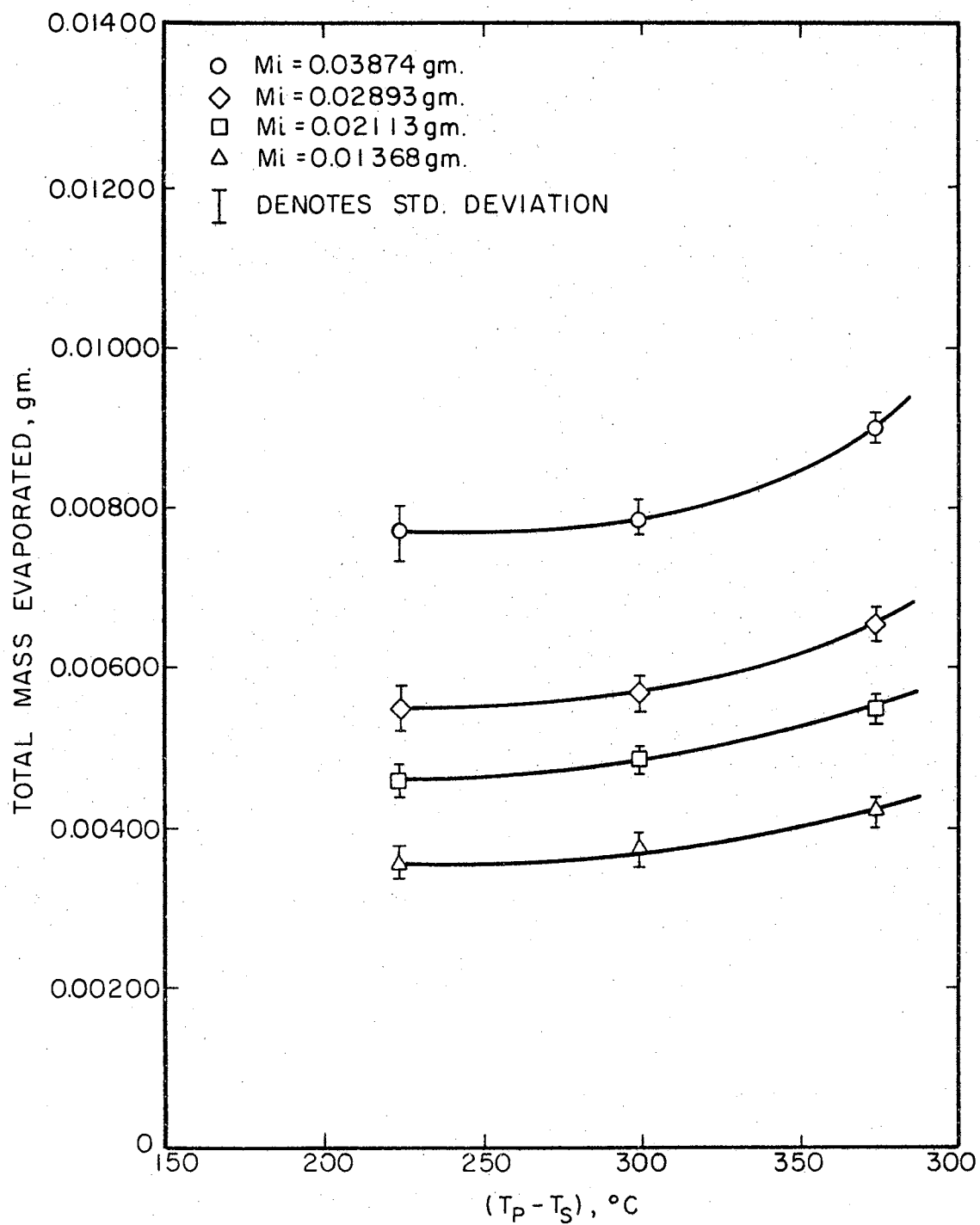


Figure 11. Evaporation of Water Droplets (Uncorrected)
(Distance traveled - 110")

APPENDIX D

CALCULATED DATA

TABLE X

WATER EVAPORATION DATA FOR FULL TUBE LENGTH (105")

Initial Mass, gm.	Mass Evaporated gm.	Initial Mass, gm.	Mass Evaporated gm.	Initial Mass, gm.	Mass Evaporated gm.	Initial Mass, gm.	Mass Evaporated gm.
0.03874	0.00774	0.02893	0.00553	0.02113	0.00463	0.01368	0.00358
	0.00824		0.00493		0.00443		0.00378
Temp., °C	0.00734	Temp., °C	0.00578	Temp., °C	0.00471	Temp., °C	0.00383
	0.00734		0.00568		0.00493		0.00323
323	0.00829	324	0.00572	324	0.00490	323	0.00323
	0.00729		0.00543		0.00453		0.00358
std. dev.	0.00754	std. dev.	0.00603	std. dev.	0.00438	std. dev.	0.00328
4.74%	0.00724	6.02%	0.00558	4.29%	0.00433	6.64%	0.00363
	0.00754		0.00539		0.00478		0.00358
	<u>0.00784</u>		<u>0.00495</u>		<u>0.00463</u>		<u>0.00393</u>
	0.00764		0.00550		0.00463		0.00357
0.03874	0.00784	0.02893	0.00553	0.02113	0.00478	0.01368	0.00388
	0.00749		0.00568		0.00488		0.00368
	0.00754		0.00588		0.00498		0.00393
400	0.00824	400	0.00593	400	0.00453	401	0.00378
	0.00804		0.00560		0.00518		0.00358
	0.00799		0.00518		0.00508		0.00398
2.84%	0.00789	4.55%	0.00613	3.39%	0.00488	4.12%	0.00383
	0.00769		0.00583		0.00473		0.00378
	0.00774		0.00588		0.00483		0.00403
	<u>0.00804</u>		<u>0.00548</u>		<u>0.00468</u>		<u>0.00353</u>
	0.00785		0.00571		0.00486		0.00380

TABLE X (Continued)

Initial Mass, gm.	Mass Evaporated gm.	Initial Mass, gm.	Mass Evaporated gm.	Initial Mass, gm.	Mass Evaporated gm.	Initial Mass, gm.	Mass Evaporated gm.
0.03874	0.00844	0.02893	0.00643	0.02113	0.00518	0.01368	0.00418
	0.00899		0.00673		0.00543		0.00433
Temp., °C	0.00884	Temp., °C	0.00628	Temp., °C	0.00533	Temp., °C	0.00428
	0.00914		0.00688		0.00573		0.00398
427	0.00919	472	0.00658	472	0.00558	472	0.00443
	0.00934		0.00648		0.00578		0.00448
std. dev.	0.00874	std. dev.	0.00688	std. dev.	0.00568	std. dev.	0.00418
1.89%	0.00894	3.14%	0.00643	3.10%	0.00553	3.22%	0.00423
	0.00909		0.00658		0.00558		0.00438
	<u>0.00889</u>		<u>0.00633</u>		<u>0.00548</u>		<u>0.00433</u>
	0.00901		0.00655		0.00552		0.00428

TABLE XI

WATER EVAPORATION DATA FOR INTERMEDIATE TUBE LENGTHS

Initial Mass, gm.	Mass Evaporated gm. (85")	Initial Mass, gm.	Mass Evaporated gm. (60")	Initial Mass, gm.	Mass Evaporated gm. (35")	Initial Mass, gm.	Mass Evaporated gm. (15")
0.03874	0.00604	0.03874	0.00454	0.03874	0.00359	0.03874	0.00269
	0.00619		0.00444		0.00374		0.00304
Temp., °C	0.00599	Temp., °C	0.00459	Temp., °C	0.00379	Temp., °C	0.00244
325	0.00629	324	0.00469	323	0.00339	323	0.00299
	0.00634		0.00429		0.00354		0.00274
	0.00594		0.00479		0.00364		0.00259
std. dev.	0.00599	std. dev.	0.00464	std. dev.	0.00344	std. dev.	0.00284
2.17%	0.00609	3.10%	0.00474	3.61%	0.00374	6.63%	0.00264
	0.00604		0.00454		0.00369		0.00279
	<u>0.00624</u>		<u>0.00449</u>		<u>0.00349</u>		<u>0.00254</u>
	0.00612		0.00458		0.00361		0.00273
0.01368	0.00308	0.01368	0.00233	0.01368	0.00178	0.01368	0.00128
	0.00293		0.00208		0.00198		0.00113
	0.00313		0.00223		0.00168		0.00133
	0.00318		0.00243		0.00193		0.00138
326	0.00303	325	0.00218	326	0.00173	326	0.00128
	0.00298		0.00213		0.00188		0.00123
std. dev.	0.00303	std. dev.	0.00248	std. dev.	0.00178	std. dev.	0.00118
3.43%	0.00313	5.39%	0.00228	6.36%	0.00183	5.64%	0.00133
	0.00323		0.00238		0.00198		0.00123
	<u>0.00288</u>		<u>0.00233</u>		<u>0.00163</u>		<u>0.00130</u>
	0.00306		0.00229		0.00182		0.00127

TABLE XI (Continued)

Initial Mass, gm.	Mass Evaporated gm. (85")	Initial Mass, gm.	Mass Evaporated gm. (60")	Initial Mass, gm.	Mass Evaporated gm. (35")	Initial Mass, gm.	Mass Evaporated gm. (15")
0.03874	0.00644	0.03874	0.00494	0.03874	0.00399	0.03874	0.00274
	0.00629		0.00479		0.00359		0.00249
Temp., °C	0.00654	Temp., °C	0.00514	Temp., °C	0.00389	Temp., °C	0.00289
400	0.00674	400	0.00519	400	0.00404	400	0.00279
	0.00639		0.00509		0.00364		0.00264
	0.00659		0.00524		0.00399		0.00259
std. dev.	0.00664	std. dev.	0.00479	std. dev.	0.00379	std. dev.	0.00264
2.21%	0.00634	2.91%	0.00489	3.99%	0.00394	4.30%	0.00279
	0.00669		0.00499		0.00374		0.00284
	<u>0.00649</u>		<u>0.00484</u>		<u>0.00369</u>		<u>0.00269</u>
	0.00652		0.00499		0.00383		0.00271

TABLE XII

BENZENE EVAPORATION DATA

Initial Mass, gm.	Mass Evaporated gm.	Initial Mass, gm.	Mass Evaporated gm.	Initial Mass, gm.	Mass Evaporated gm.	Initial Mass, gm.	Mass Evaporated gm.
0.01458	(105")	0.01148	(85")	0.00937	(60")	0.00589	(60")
	0.00983		0.00623		0.00462		0.00344
	0.00948		0.00640		0.00407		0.00349
Temp., °C	0.00963	Temp., °C	0.00678	Temp., °C	0.00422	Temp., °C	0.00349
325	0.00983	324	0.00656	324	0.00427	324	0.00359
	0.00913		0.00629		0.00447		0.00329
std. dev.	0.00998	std. dev.	0.00618	std. dev.	0.00412	std. dev.	0.00319
2.51%	0.00978	3.10%	0.00640	4.76%	0.00397	3.92%	0.00364
	0.00958		0.00662		0.00432		0.00334
	0.00988		0.00651		0.00442		0.00349
	<u>0.00943</u>		<u>0.00612</u>		<u>0.00402</u>		<u>0.00354</u>
	0.00966		0.00641		0.00425		0.00344

VITA

DANIEL ALAN FORBES

Candidate for the Degree of

Master of Science

Thesis: FILM BOILING OF SMALL LIQUID MASSES IN MOTION ON A HEATED SURFACE

Major Field: Chemical Engineering

Biographical:

Personal Data: Born in Pampa, Texas, April 18, 1946, the son of John N. and Thelma Forbes. Married to Sheila Harris, September, 1966.

Education: Attended elementary school in Ardmore, Oklahoma; attended high school in Elk City, Oklahoma; graduated from Elk City High School in 1963; received a Bachelor of Science degree from Oklahoma State University in July, 1967; completed requirements for Master of Science degree at Oklahoma State University in July, 1968. Membership in scholarly or professional organizations includes Phi Kappa Phi, Omega Chi Epsilon, and American Institute of Chemical Engineers.

Professional Experience: Summer employment with Shell Oil Company, Woodward, Oklahoma, 1964; summer of 1965, with Shell Oil Company, Denver City, Texas; summer of 1966, with Development Department, Phillips Petroleum Company, Bartlesville, Oklahoma. Presently employed by Continental Oil Company, Ponca City, Oklahoma.